

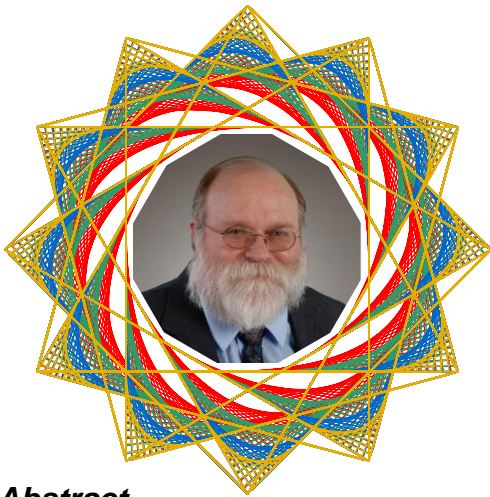
# Humanistic Explorations in Algorithmic Art using Sequence Player mode of *Playing with Polygons*

Prof. Stephen Erfle, PhD.

Department of International Business and Management, Dickinson College, Carlisle, PA USA

<https://blogs.dickinson.edu/playing-with-polygons/>

e-mail: [erfle@dickinson.edu](mailto:erfle@dickinson.edu)



## Abstract

Electronic string art is algorithmic art in which images change instantaneously as users change parameters of the model. This interactive play allows users to test hypotheses even if those hypotheses are only incompletely understood. The *Sequence Player* mode increases the dynamism involved in such play and hence increases the likelihood that the user will test additional hypotheses. Such purposeful play leads to learning, even if that learning is informal in nature.

## 1. Background

*Electronic String Art*, ESA, simulates traditional string art which creates intricate patterns based on a simple

counting rule (connect every 7<sup>th</sup> nail with string) on a closed set of vertices based on four parameters:  $n$  and  $J$  create the  $n, J$ -star vertex frame, VF;  $S$  is the number of equally spaced endpoints (think nails) on each line of the VF, and  $P$  is the counting rule using these endpoints to connect lines in the final image [1]. Two electronic modalities of image creation are available, Excel, and a web version developed by Liam Myles [2]. These basics are laid out in [3] in which I argued that ESA can be used as an educational resource up and down the K-12 curriculum.

Due to the simplicity of the underlying model, ESA can be used as a teaching tool, or more generally as an informal learning resource. The four parameters can be adjusted using up and down arrows which allows even young users the ability to play and see what happens. This discovery process is consistent with Stein's *Triex: Explore, Extract, Explain* view of how one can more deeply teach and understand mathematics [4].

An open question is how artificial intelligence, AI, will change the nature of education: What should be taught and how, as well as what needs to be understood to be a productive citizen in this rapidly changing world? How will we maintain our human imprint in a

technologically assisted world?

Two themed issues of the *Bulletin of the American Mathematical Society (New Series)*, April and July 2024, examine how AI technology is likely to affect the work of research mathematicians. In one article, Davis notes that despite progress on many fronts, AI has, to this point, failed to surmount the intricacies of elementary mathematical word problems [5]. As U.C. Davis Emeritus Professor Don Chakerian stated in email discussion on this topic [6]: “The article by Davis shows how children can outstrip the most powerful AI systems we have now in dealing with very elementary word problems. You could mention the even greater contrast in the creativity of children in making aesthetic judgments regarding visual figures and patterns. Machines calculate, but humans evaluate. Machines not only lack creativity, but also a sense of play and recreation!”

The present paper focuses on simple regular polygons and stars. By this we mean that the VF will be a triangle, square, or a simple  $n, J$ -star like a pentagram or a 12,5-star, or variations on these simple images in the sense that the images will have rotational symmetry of  $120^\circ$ ,  $90^\circ$ ,  $72^\circ$ , or  $30^\circ$ , for example.

Regular divisible stars cannot be created in ESA due to the *continuously drawn* nature of the ESA images but “close to” divisible star images such as the 492-line 12,3 and 12,4 images in Fig 1 are possible. Both are based on a regular 12,5 VF star. The upper image has three “squares” tilted  $30^\circ$  to one another. The lower image has four “equilateral” triangles tilted  $30^\circ$  to one another. Both are readily understood based on how

close their respective  $P$  values are those producing a square,  $P = 492/4 = 123$ , and equilateral triangle,  $P = 492/3 = 164$ .

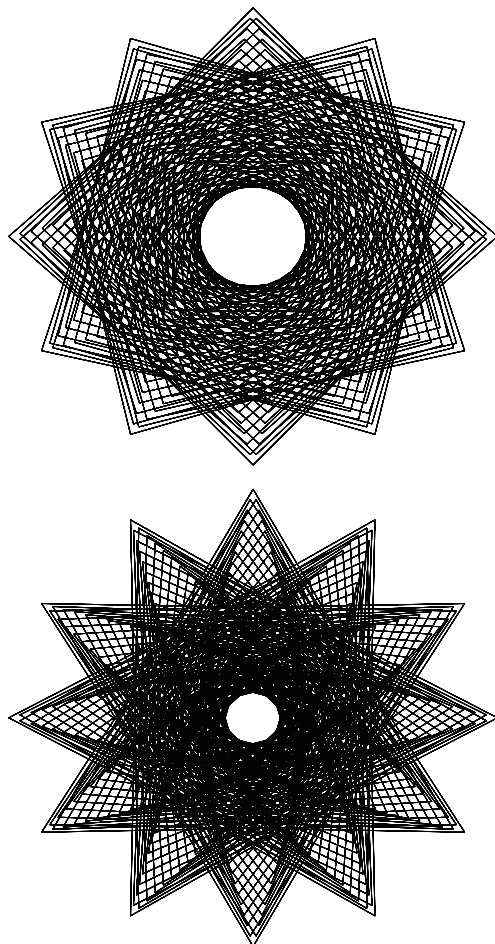


Fig 1. Two almost regular 492-line stars given  $n = 12$ ,  $S = 41$ ,  $J = 5$ . Upper 12,3-star,  $P = 121$ ; Lower 12,4-star,  $P = 163$ .

The images in Fig 1 are two of 80 distinct full density images available given these values of  $n$ ,  $S$ , and  $J$ . As the counting rule  $P$  varies for fixed  $n$ ,  $S$ , and  $J$  one obtains waves of images punctuated by images with fewer lines. ESA Sections 10.2 and 18.5 describe why waves of images appear to adjust smoothly as  $P$

changes unless the number of lines in the image changes in which case the image sequence seems to flicker relative to surrounding images. Put another way, as noted in ESA Section 5.4, the images are full density (all subdivisions are used) unless  $SCF = \text{GCD}(P, S \cdot n / VCF) > 1$ . This observation forms the basis for the *Sequence Player* mode to which we now turn.

## 2. Sequence Player Mode

One form of dynamism, discussed in [1,3] using the *Home* mode of [2] is how an individual image is drawn as a series of connected line segments given fixed  $n$ ,  $S$ ,  $P$ , and  $J$ . This is the notion of being *continuously drawn*. The present paper focuses on a second form of dynamism: How do images change as the counting rule changes? This can be examined manually using *Home* mode by adjusting  $P$ , but it is automated in the *Sequence Player* mode. Two additional modes are available from [2], *Picked Sequences* provides a library of *Sequence Player* image sequences (click to activate), and *Spirals* is discussed elsewhere [7,8].

To avoid the flickering that occurs when  $SCF > 1$ , all images in a *Sequence Player* sequence are full density,  $SCF = 1$  (except the *Start Points*  $P$  which can have any value of  $SCF$ ). The *Start Points*  $P$  value can be chosen to make a point, but if  $SCF > 1$ , it will not be shown in subsequent image sequence iterations. When *Speed* is at its default value of 100, approximately 10 images are shown per second.

Regardless of initial *Start Points* value, if  $n$ ,  $S$ , or  $J$  changes,  $P$  is reinitialized to 1. The maximum  $P$  is set to  $n \cdot k \cdot S$  since the maximum number of lines for images in a sequence,  $\mathbf{N}$ , is  $\mathbf{N} = n \cdot k \cdot S / VCF$  and  $k$  is

the number of jumps in a jump set. *The number of lines in in the image,  $\mathbf{N}$* , changes because  $VCF$  changes as  $J$  changes. The general rules for lines in the VF with jump sets is  $k \cdot n / VCF$  with  $VCF = \text{GCD}(J, n)$  and *the jump set sum is  $J = J_1 + J_2 + \dots + J_k$* . In the jump set context,  $SCF = \text{GCD}(P, \mathbf{N})$ .

## 3. The Total Number of Images in a Sequence, T

Some  $P$  values between 1 and  $\mathbf{N}$  have  $SCF > 1$  and therefore are not included in an image sequence. Values of  $P$  included in the image sequence are coprime to  $\mathbf{N}$ , or  $SCF = 1$ .

### 3.1 The Single Prime Case

If  $\mathbf{N}$  has a single prime factor,  $a$ , then all  $P$  from 1 to  $a-1$  are coprime to  $\mathbf{N}$  as are  $a+1$  to  $2a-1$ , and so forth. This implies that *the total number of full density images is  $T = \mathbf{N} \cdot (a-1) / a$* . Figs 2 through 4 show examples based on the first three primes, chosen because each sequence has roughly 500 images. See **NOTES** for a link to each figure's image sequence.

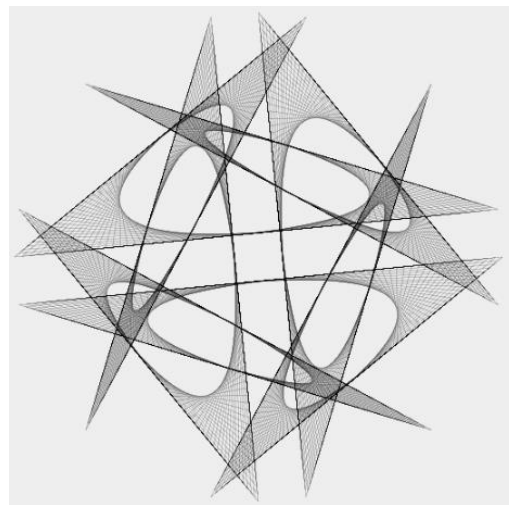


Fig 2. An image based on powers of 2.

Fig 2 has  $n = 32$  but  $VCF = 8$  so one can readily see the four-ness in the resulting image, due to  $90^\circ$  rotational symmetry. This  $2^{10} = 1024$ -line image is a *curved-tip star* [1] because  $P < S$  making the four-jump set pattern (9,19,11,17) easy to follow. Note the four different sized nested squares outlined as a result. The image shown is one of 512 images in the sequence because every odd number is coprime to 1024,  $512 = 1024 \cdot (2-1)/2$ .

Fig 3 has  $n = 27$  but  $VCF = 9$  so the resulting curved tip star image certainly exhibits three-ness or  $120^\circ$  rotational symmetry. The 9-line VF has an internal equilateral triangle and two truncated equilateral triangles [7] due the three-jump set pattern of (6,10,2). This  $3^6 = 729$ -line image is one of 486 in the image sequence because  $486 = 729 \cdot (3-1)/3$ .

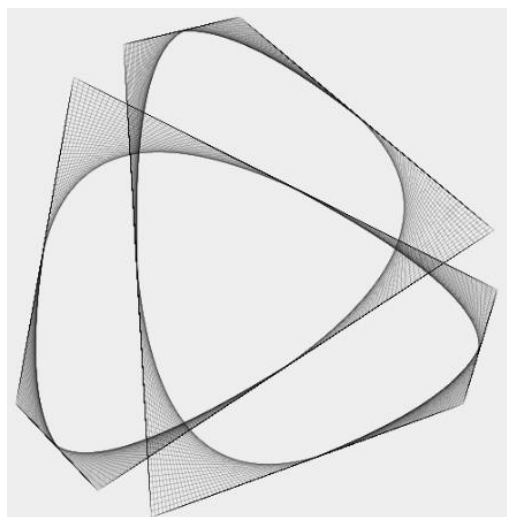


Fig 3. An image based on powers of 3.

Fig 4 has  $n = 25$  but  $VCF = 5$  so the resulting image certainly exhibits five-ness or  $72^\circ$  rotational symmetry. This image uses a five-jump set pattern of (8,1,25,22,4). Note the middle jump is a zero jump [1,3] which is why there is a

spray of lines at vertices 4, 9, 14, 19, and 24. This  $5^4 = 625$ -line image is one of 500 in the sequence,  $500 = 625 \cdot (5-1)/5$ . Indeed,  $P = 312$  is the *porcupine* image [1]; note that  $P = 313 = 625-312$  is the same static image drawn in reverse.

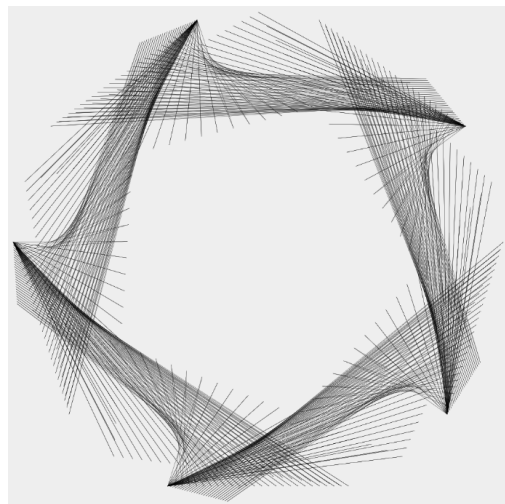


Fig 4. An image based on powers of 5.

### 3.2 There is symmetry about the porcupine value of $P$

Although there are 500 images in the Fig 4 image sequence, only half are distinct. The  $P < N/2$  and  $P > N/2$  halves are always the same images shown in reverse order. Seeing the images in reverse order may make it appear like they are different images, but this is only an optical illusion. It is always the case that for  $P < n$ ,  $P$  and  $n-P$  produce the same static image drawn in reverse [1].

It is worth noting that porcupine images have a different look when  $n$  is even from when  $n$  is odd. Fig 5 shows the  $P = 245$  porcupine image based on the Fig 1 image sequence. Note the prickly 12,5-star nature of this image. Fig 6 shows the  $P = 511$  porcupine image based on the

Fig 2 four-jump set image sequence. The Fig 7 triangular porcupine,  $P = 364$ , is based on the Fig 3 three-jump set image sequence.

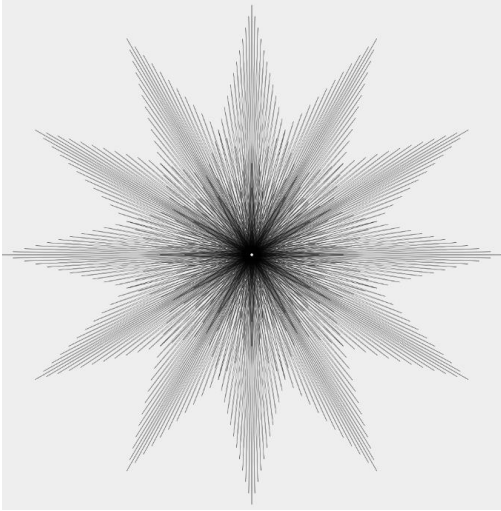


Fig 5. Porcupine 12,5-star for Fig 1.

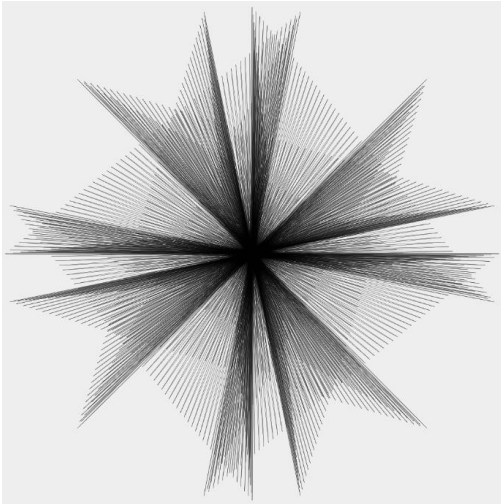


Fig 6. Complex porcupine for Fig 2 with  $90^\circ$  rotational symmetry.

The similarity between even  $n$  Figs 5 and 6 porcupines and odd  $n$  Figs 4 and 7 porcupines is clear. Since Figs 5-7 are based on Figs 1-3, use the links to those

images at **NOTES** and change  $P$  as necessary.

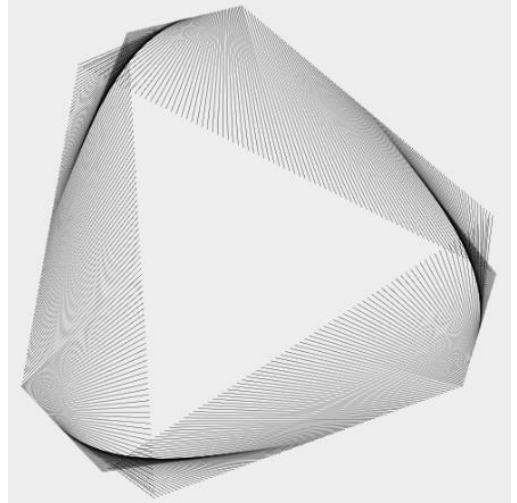


Fig 7. Porcupine image for Fig 3.

### 3.3 The General Rule for T

Suppose  $\mathbf{N}$  has  $r$  distinct primes,  $r > 1$ , labelled  $a_1, a_2, \dots, a_r$ . Of this number, the fraction  $(a_1-1)/a_1$  are coprime to  $a_1$ , the fraction  $(a_2-1)/a_2$  of those remaining are coprime to  $a_2$ , and so on. The total number of  $P$  values that are coprime to all  $r$  primes,  $\mathbf{T}$ , is thus:

$$\mathbf{T} = \mathbf{N} \cdot (a_1-1)/a_1 \cdot (a_2-1)/a_2 \cdot \dots \cdot (a_r-1)/a_r \quad (1)$$

We noted above that Fig 1 showed 2 of 80 possible full density images given  $n$ ,  $S$ , and  $J$ .  $\mathbf{N} = 12 \cdot 41 = 492$  has three prime factors, 2, 3, and 41. Total images,  $\mathbf{T} = 160 = 492 \cdot (2-1)/2 \cdot (3-1)/3 \cdot (41-1)/41$  according to Equation (1) but half, or 80, are distinct due to symmetry about the porcupine value discussed in Section 3.2.

### 3.4 Waves of Images

Sometimes image sequences do not appear to morph smoothly as  $P$  increases. This occurs when there are not enough full density images in a

sequence,  $T$ , but the notion of “enough” cannot be crisply defined. Nonetheless, we can see why waves are more likely to appear smooth if fewer primes are used, or if they are larger primes.

Fig 8 provides four similar images; each is an example of *polygons in a cycle* discussed in ESA Section 10.5 [1]. Each is a part of an image sequence but 8a uses 4 primes, 8b uses 3, 8c uses 2 and 8d uses 1. The percentage of  $N$  (210, 195, 225, 169 in 8a-8d) used increases from 22.9% to 49.2% to 53.3% to 92.3% in going from 8a to 8d. If you watch the image sequences for each (using the links at **NOTES**), you will see smoothness increase in going from 8a to 8d because 8d has the most images,  $T = 156$ , despite having the smallest number of lines per image,  $N = 169$ .

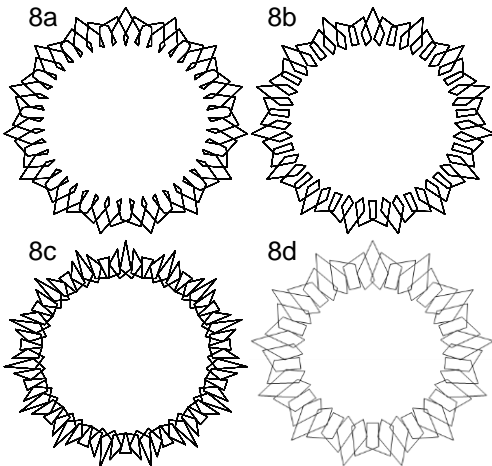


Fig 8. 8a-(15,14,53,4), 8b-(15,13,49,4), 8c-(15,15,56,4), 8d-(13,13,42,4).

One obtains even smoother image transitions if  $S$  is a larger prime. Fig 9 shows the porcupine image in that image sequence. This sequence was chosen because it has roughly the same  $N = 185$  and  $T = 144$  as Fig 8 sequences. This  $T$

is smaller than in 8d, but the sequence appears to morph more smoothly because the number of endpoints on a VF line,  $S$ , is 37 rather than 13. Note also that Fig 1 morphs smoothly with  $T = 160$  because  $S = 41$ .

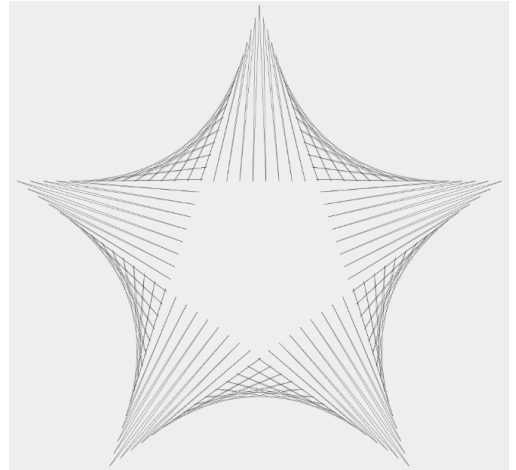


Fig 9. A 5,2-star porcupine image.

#### 4. Elementary Questions

The 12,5-star image sequence used to create Figs 1 and 5 is the default image sequence for *Sequence Player* mode. By adjusting  $J$  one can readily use this image sequence to explain common divisors. Reduce  $J$  by 1 to 4 and a triangle VF results because 12 and 4 have 4 in common; a triangular image results if we skip count by 4s (4, 8, 12). Reduce  $J$  again and we have a square because 12 and 3 have 3 in common; a square VF results if we skip count by 3s (3, 6, 9, 12). This process can be pushed in various ways by varying both  $J$  and  $n$  to examine common factors. For example, set  $J = 2$ , vary  $n$  and watch an alternation between  $n,2$ -stars, and  $n/2$  polygons. All of this is done while having a mesmerizing image sequence play out in the background.

## 5. Equilateral Three-ness

From an educational perspective, the best question you can ask is: *Can you find similar but not identical images to an image you find interesting?*

Our interest here is in finding image sequences that exhibit  $120^\circ$  rotational symmetry or *equilateral three-ness*. Fig 10 reduces  $S$  from 81 to 27 relative to Fig 3 so that the image sequences do not take as much time to view. Each  $3^5 = 243$ -line sequence has 162 images as a result.

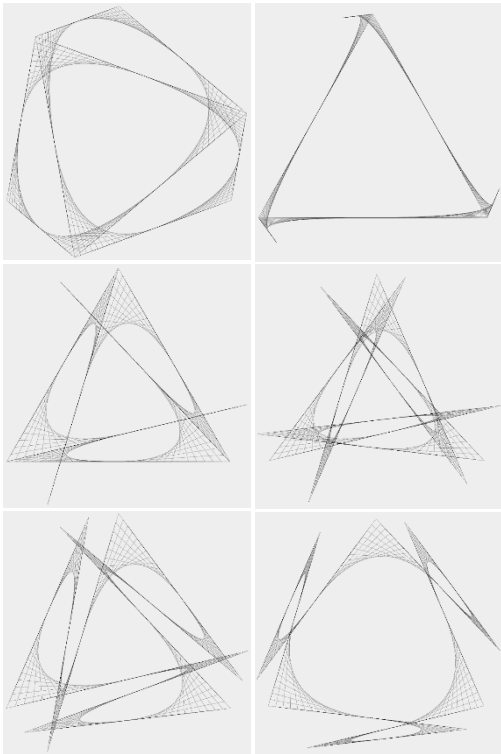


Fig 10. A sampling of image sequences with equilateral three-ness. Each image shown is  $P = 14$ . Links are Top 10a, 10b, Middle 10c, 10d, and Bottom 10e, 10f.

The first three versions, 10a-10c, have inscribed equilateral triangles that include

vertices of the 27-gon because one of the jumps in the jump set is  $9 = n/3$ . Fig 10d has three interior VF equilateral triangles, Fig 10e has two interior and one truncated VF equilateral triangles and all three of the Fig 10f VF triangles are truncated [7]. Figs 10b and 10c are examples of tails and spikes discussed in ESA Section 17.3 [1]. Note also that 10d and 10e are obtained from 10c by adjusting  $J_1$  up or down 1 and  $J_2$  down or up 1 relative to 10c. Doing so changes the  $0^\circ$  spike into a  $180/27 = 6.67^\circ$  sharp angle according to the inscribed angle theorem.

The image sequences in Fig 10 are not exhaustive, but simply are examples of some of the possibilities given  $n = 27$  and  $k = 3$ . Of course, other values of  $n$  produce similar equilateral three-ness images (and different ones), all that is required is that  $n$  is a multiple of 3 and  $3 = n/VCF$ . The images in Fig 10 worked because  $VCF = 9$  in each case and one need only adjust jumps in the jump set to find additional versions.

Equilateral four-ness, or  $90^\circ$  rotational symmetry, is similarly easy to obtain. One need only have  $n$  be divisible by 4 with  $4 = n/VCF$ . From here you might challenge students to create images that have 5,2-ness, or 7,3-ness.

## 6. Extensions

As you adjusted jumps in a three-jump set you may have run across situations where a scalene triangle results. This happens whenever the sum of jumps is a multiple of  $n$ . This forms the basis for obtaining “closest to equilateral” triangles when  $n$  is not divisible by 3.

Figs 11a and 11b show the smallest  $n$  isosceles, but not equilateral, porcupine

images where the difference in angles is less than  $1^\circ$  (the difference is  $180/181^\circ$  and  $180/182^\circ$ , respectively). The apex angle of 11a is greater than  $60^\circ$  and 11b is less than  $60^\circ$  but both are virtually indistinguishable from [\(3,81,121,1\)](#).

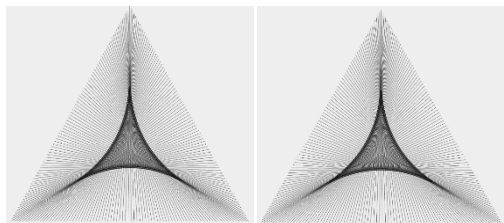


Fig 11. Two isosceles porcupines.

## 7. Summary

*Electronic String Art* combines art and mathematics in a way that allows users to understand mathematics more deeply, simply by adjusting parameters and watching what happens. The *Sequence Player* mode of *Playing with Polygons* provides a dynamic complement to the *Home* mode that helps users understand how individual images emerge as a result of applying a simple counting rule. Both modes were created for independent explorations, but both are useful in more formal K-12 classroom settings to support teaching of various topics in a visually appealing way.

## Notes

Each link takes you directly to the web version [2] set to that figure in *Sequence Player* mode. Links to Figs 1-9 note the number of lines in the image, **N**, and the number of images in a sequence, **T** and starting *P* as **N, T, P**. Figs 10 and 11 note the jump set associated with each panel.

[Fig 1](#),492, 160, 121. [Fig 2](#),1024, 512, 37.

[Fig 3](#),729, 486, 47. [Fig 4](#),625, 500, 312.

[Fig 8a](#),210, 48, 53. [Fig 8b](#), 195, 96, 49.

[Fig 8c](#),225, 120, 56. [Fig 8d](#),169, 156, 42.

[Fig 9](#),185, 144, 92.

[Fig10a](#) (6,9,3). [Fig 10b](#) (9,26,1).

[Fig 10c](#) (9,16,11). [Fig 10d](#) (10,15,11).

[Fig 10e](#) (8,17,11). [Fig 10f](#) (7,21,8).

[Fig 11a](#) (60,61,60). [Fig 11b](#) (61,60,61).

## References

- [1] S. E. Erfle, *Electronic String Art: Rhythmic Mathematics*, [2024](#).
- [2] L. Myles, "Playing with Polygons." <https://www.playingwithpolygons.com/>.
- [3] S. E. Erfle, "Electronic String Art as Educational Algorithmic Art." *XXVII Generative Art Conference, 2023*, Celestino Soddu, Editor. Rome, Italy. ([10 page paper](#))
- [4] S. K. Stein, "The Triex: Explore, Extract, Explain." *Humanistic Mathematics Network Journal*, vol. 1, no. 14, pp. 6–8, [1996](#).
- [5] E. Davis, "Mathematics, Word Problems, Common Sense, and Artificial Intelligence." *Bulletin of the American Mathematical Society (New Series)*, vol. 61, no.2, April 2024, pp. 287-303.
- [6] D. Chakerian, email communication, May 19, 2024.
- [7] S. E. Erfle, "Playing with Polygons." <https://blogs.dickinson.edu/playing-with-polygons/>.
- [8] S. E. Erfle, "Using Archimedean Spirals to Explore Fractions." *Proceedings of Bridges 2021: Mathematics, Art, Music, Architecture, Culture*, pp. 397-402, [2021](#).